

Electronic Supplementary Information

Atmospheric Pressure Chemical Vapor Deposition of High Silica SiO₂-TiO₂ Antireflective Thin Films for Glass Based Solar Panels

Erik R. Klobukowski,^a Wyatt E. Tenhaeff,^a James W. McCamy,^b Caroline S. Harris,^b and Chaitanya K. Narula*^a

^a Materials Science & Technology Division, Oak Ridge National Laboratory, P.O. Box 2008, Oak Ridge, TN 37831-6133 E-mail: narulck@ornl.gov

^b Solar Performance Group, PPG Industries, Cheswick, PA 15024-9464

Experimental Section

Materials & Methods

Tris-*tert*-butoxysilanol, titanium tetrakis-isopropoxide, and hexanes (a mixture of isomers) were purchased from Sigma Aldrich. Tris-*tert*-butoxysilanol was used as received. Titanium isopropoxide was distilled under reduced pressure and hexane was distilled from sodium benzophenone ketyl prior to use.

Synthesis of [(⁴BuO)₃SiO]₂-Ti(OⁱPr)₂]

Reactions were setup by loading tris-*tert*-butoxysilanol (2.00 g, 7.57 mmol) to an addition funnel that was inserted into a 2-neck flask equipped with a J. Young high-vacuum valve and drying overnight under reduced pressure. The tris-*tert*-butoxysilanol was dissolved by adding 25 ml hexanes to the addition funnel. The flask was charged with 1.11 mL titanium isopropoxide (1.07 g, 3.88 mmol) and 20 ml hexanes. The tris-*tert*-butoxysilanol solution was then added dropwise over 1 hour to the flask containing the titanium isopropoxide solution. All additions and manipulations were done under either a nitrogen or argon environment. The mixture was then allowed to continue to stir for an additional hour. The volatiles were then removed under reduced pressure. The titanatosiloxane was then injected into the APCVD reactor bubbler and backfilled with nitrogen.

Thin Film Deposition

The schematics of the APCVD reactor assembled in our laboratory are shown in Figure S1.

A high transmittance (low iron) float glass sheet was cut into 5/8" x 3/4" coupons which cleaned using a 1:1 ²ProOH/H₂O mixture. The clean glass coupon was then placed into a ceramic slide that contained a slit that allowed the coupon to rest at 30°. After inserting the slide into a split-hinge Lindberg/Blue M tube furnace, the reactor was then dried under vacuum for 10 minutes, after which ultra high-purity nitrogen (99.999% purchased from Air Liquide) was then introduced and it was heated to the desired deposition temperature. The precursor bubbler was heated to 100 °C using an oil bath. The lines leading to the reactor were kept at 125 °C to prevent condensation of the precursor. The flows of the carrier and dilution gases were controlled using mass flow controllers. After the furnace, bubbler, and lines had reached their appropriate temperatures, valves were opened to allow for heated carrier gas to be delivered to the bubbler. After the desired deposition time, the carrier and dilution gases were turned off and the slide was removed after the furnace had cooled.

Characterization

The samples of [(⁴BuO)₃SiO]₂-Ti(OⁱPr)₂] were characterized using ¹H and ¹³C NMR and FTIR spectroscopy. ¹H and ¹³C NMR experiments were run on either a 400 MHz Bruker Avance III or Avance 400 spectrometer. All samples

were dissolved in d-chloroform that was dried over 4Å molecular sieves. The IR was recorded from a thin film of $\text{[}(\text{BuO})_3\text{SiO}]_2\text{-Ti(O}^{\text{i}}\text{Pr)}_2\text{]}$ on a NaCl window. Elemental analysis was performed by Galbraith Laboratories, Knoxville, TN. The characterization data are presented in the manuscript.

The film thickness and refractive index were analyzed using a JA Woollam M-2000U spectroscopic ellipsometer and fitted using the Cauchy model ($n(\lambda) = A + B/\lambda^2 + C/\lambda^4$) at 632 nm. The thin films were scanned from 400 - 1000 nm at three angles of incidence (65, 70, 75°) to confirm homogeneity of films. The $\text{SiO}_2\text{:TiO}_2$ content of the films were analyzed using a PHI 3056 XPS instrument with an Al anode source operated at 15 kV and an applied voltage of 350 W at a vacuum chamber pressure $< 10^{-8}$ torr. Scans were measured at 93.9 eV pass energy, 0.5 eV energy step, and 20 repeats. The film absorbance was measured using an Ocean Optics UV-Vis spectrometer. The film surface was also analyzed by XRD, but no new peaks were observed after the film had been deposited which is not surprising since it has been previously reported that conventional XRD does not have the appropriate sensitivity to typically analyze films with thicknesses less than 500 nm.¹

Table S1 summarizes characterization data that show the effect of deposition temperature on $\text{SiO}_2\text{:TiO}_2$ ratio and refractive index. Table S2 and S3 show the effects of deposition time and gas flow on film thickness.

References:

- 1 B. A. Van Brussel, J. T. M. DeHosson, *Appl. Phys. Lett.*, 1994, **64**, 1585.

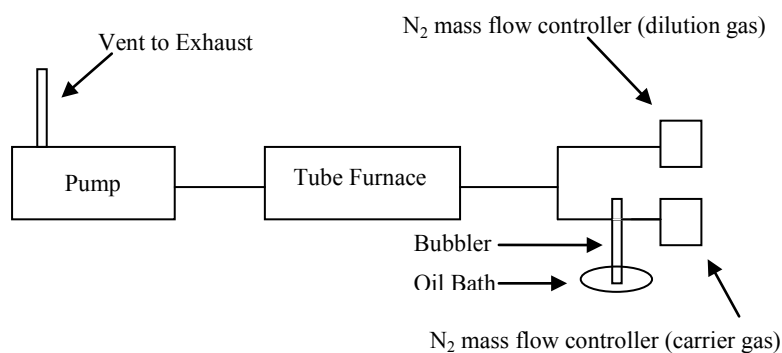


Fig. S1: Schematic Diagram of APCVD Instrument

The SiO₂:TiO₂ ratios were measured using XPS and the refractive index and film thickness were analyzed using spectroscopic ellipsometry and fitted using the Cauchy model.

Table S1: Effect of Deposition Temperature on SiO₂:TiO₂ ratio and refractive index*

Sample	Deposition Temperature (°C)	SiO ₂ :TiO ₂ Ratio	Refractive Index (632 nm)
1	450	2.39	1.73
2	500	2.56	1.72
3	550	2.97	1.69
4	600	3.73	1.63

*Conditions: Deposition Time (20 min), Carrier Gas Flow (1000 sccm), Dilution Gas Flow (2500 sccm)

Table S2: Effect of Deposition Time on Film Thickness*

Sample	Deposition Time (Minutes)	Thickness (nm)	Refractive Index (632 nm)
1	10	49	1.61#
2	20	110	1.66
3	40	184	1.68
4	60	295	1.66

*Conditions: Deposition Time (500 °C), Carrier Gas Flow (1000 sccm), Dilution Gas Flow (2500 sccm)

#Since the thickness of the film is considerably less in Sample 1, it is possible that any differences in uniformity of this sample, are more pronounced, which could contribute to a lower calculation of the refractive index.

Table S3: Effect of Deposition Time on Film Thickness at faster carrier and dilution gas flow*

Sample	Deposition Time (Minutes)	Thickness (nm)
1	1	19
2	2.5	93
3	5	183
4	10	343

*Conditions: Deposition Temp (500 °C), Carrier Gas Flow (5000 sccm), Dilution Gas Flow (1000 sccm)